

Restoration of vision IV: role of compensatory soma swelling of surviving retinal ganglion cells in recovery of vision after optic nerve crush

V. Rousseau and B.A. Sabel*

Institute of Medical Psychology, Medical Faculty, Otto-v.-Guericke University of Magdeburg, 39120 Magdeburg, Germany

Received 1 May 2001; revised 8 October 2001; accepted 15 October 2001

Abstract

Purpose: Diffuse axonal injury following partial optic nerve crush (ONC) leads to severe visual deficits from which rats can partially recover within 2-3 weeks. To evaluate the role of surviving retinal ganglion cells (RGCs) in recovery, we have observed their morphology repeatedly *in vivo* with ICON-microscopy and correlated cell size changes with recovery of vision which we observed in parallel in the same animals.

Methods: After rats had learned a visual contrast discrimination task using an automated, computer-based test, RGCs were labeled retrogradely with fluorescent beads. Animals then received either no lesion, a complete axotomy or bilateral mild, moderate or severe ONC. Before surgery and for 40 days post-operatively, RGC number and soma size was repeatedly quantified every five days with the *in vivo* confocal neuroimaging method (Sabel et al., *Nature med.* 3, 1997, p. 244). In parallel, visual function was quantified with the contrast-discrimination task.

Results: After ONC about 70 % of the RGCs died after having undergone a fast and massive soma swelling. The extent of cell death was independent of crush severity. RGCs surviving the injury did not change their body size over time in the severe group and these animals also did not recover their vision. In contrast, after a mild or moderate crush, about half of the surviving RGCs experienced a slow and moderate, "compensatory" cell soma swelling and the rats showed partial recovery of vision. Both the number of RGCs showing such compensatory soma swelling and the extent of the swelling correlated highly ($r = 0.96$) with recovery of contrast discrimination performance at post-operative days 23 and 38.

Conclusions: Depending on the time course and extent, soma swelling after neurotrauma may be associated either with cell death or recovery of function. Because of the very high correlation between extent of recovery and amount of soma swelling, moderate soma swelling contributes in a prominent way to recovery of vision. We believe that these cells provide an important structural substrate for neuronal tissue repair and therefore term these cells "compensatory neurons".

Keywords: vision, plasticity, retinal ganglion cells, recovery of function, recovery of vision, ICON, contrast discrimination, neurotrauma, rat

1. Introduction

Despite diffuse axonal injury (DAI) following neurotrauma [18,33,38], the injured brain has a remarkable potential to recover neurological and neuropsychological functions [13,14,15,49]. While great efforts are underway to under-

stand the mechanisms of DAI soon after the injury [33], little is known about the later recovery phase, which takes places over the course of weeks and months thereafter. Because, from a clinical perspective, it is desirable to be able to predict and manipulate recovery of function, the mechanisms of plasticity and repair need to be explored.

Partial optic nerve injury has been proposed as a model to simulate DAI. Both optic nerve stretch [19] and partial crush have been studied physiologically, morphologically and behaviorally [9,29,46,45,48]. It was found that following par-

* Corresponding author: Dr. Bernhard A. Sabel, Institute of Medical Psychology, Otto-v.-Guericke University of Magdeburg, Leipzigerstr. 44, 39120 Magdeburg, Germany. Tel.: +49 391 611 7100; Fax: +49 391 611 7103; E-mail: Bernhard.Sabel@Medizin.Uni-Magdeburg.de.

tial optic nerve crush (ONC), recovery of vision occurs 2–3 weeks following injury [45] despite a cell survival rate of only about 10–20 % [41,46].

Because such a small number of cells is apparently sufficient for remarkable recovery of vision [45,46], it is of particular interest to determine if and how surviving cells may change morphologically and how such changes contribute to the recovery process. However, to date it has not been possible to correlate *in vivo* morphological changes of surviving retinal ganglion cells (RGCs), such as cell number and size, with visual performance. We have therefore developed the *in vivo* confocal neuroimaging (ICON) technique [43] that permits observations of RGCs in the living rat eye. With the ICON technique, which utilizes the confocal laser scanning microscope in conjunction with a contact lens, RGCs can now be imaged non-invasively and repeatedly *in vivo*. The resolution of ICON is sufficient to identify individual cells and their diameters.

We have already shown with ICON that a moderate and slow, but not fast and severe, RGC soma swelling anticipates cell survival [40]. Because cells with moderate swelling recover their soma diameter expansions, we have also proposed moderate cell swelling to be an adaptive response that may help traumatized central nervous tissue to repair itself. But because no relationship had been established between such morphological parameter and functional measures, the final proof of this claim was still outstanding.

The study presented here was therefore carried out to determine if compensatory cell soma swelling indeed contributes to recovery of vision. By taking advantage of ICON's ability to repeatedly observe RGCs in the same animal over time, we studied in parallel RGC soma swelling dynamics and recovery of contrast discrimination performance in the living rat after optic nerve crush. We now report that compensatory RGC soma swelling correlates highly with recovery of visual functions, suggesting that both processes are causally related.

2. Methods

Prior to the experiments ethical approval was obtained according to requirements of the German National Act on the Use of Experimental Animals.

2.1. Subjects

Hooded rats (BDE-Han strain, age: 10 weeks) were kept, two per cage, on a 12–12 h dark-light cycle at a relative humidity of 50–60 % and 22 °C with food available *ad libitum*.

2.2. Behavioral testing

Before ONC surgery, rats were trained on a contrast discrimination apparatus (see below) until they reached a predetermined performance criterion. After ONC, visual performance was tested daily, starting on post-operative day 1 (P1) through day 40 (P40).

Before training was initiated, rats were handled 10–15 min daily and, at the same time, they were water deprived. Water deprivation was achieved by withdrawing water for 24 h on the first day, with 15 min water access daily thereafter until the rats reached 80–90 % of their *ad libitum* body weight (which takes about 1 week). During the post-operative testing period, 15 min water access was allowed daily after the testing session had been completed.

Contrast discrimination apparatus: Animals were trained on an automated visual testing apparatus described previously [27]. Briefly, this apparatus is a modular chamber (Coulbourn Instruments, USA) equipped with a dipper with one side of the chamber containing a 6-stimulus location arrangement (a 2 × 3 array) centered in the wall opposite from the water dipper. Here, a 14" VGA monitor was used to present visual stimuli at each of these 6 locations: five S-stimuli and one S+ stimulus.

The stimuli were vertically oriented achromatic sine-wave contrast gratings. Grating contrast was defined in Michelson units: $C = (L_{\max} - L_{\min}) / (L_{\max} + L_{\min})$, where L_{\max} and L_{\min} are the grating's maximum and minimum luminance values, respectively. The contrast values used for testing were 6 %, 10 %, 15 %, 20 %, 30 %, 45 %, 50 %, 60 %, 75 % and 96 %. Mean luminance was 32 cd/m². A spatial frequency of 0.14 cyc/deg, known to be within the rat's range of sensitivity, was used for all stimuli. The position of S+, i.e. the contrast grating pattern, varied randomly and five S-stimuli, i.e. gray surfaces equal in luminance to the grating mean, served as distractors.

Training schedule: All training and testing took place within a dark, sound attenuating room. Sessions lasted approximately 45 min for each rat. The rats showed little motivational loss during the respective sessions.

Initial training involved establishment of the reinforcer and behavioral shaping to nose poke. A maximum-contrast grating was used for the training phases. Shaping involved a session displaying a grating (the remaining positions were devoid of stimuli) that varied randomly in position, with simultaneous presentation of S- which, at this point, had a luminance equal to background. Following a short period of adaptation to the chamber, the reinforcer was established by manually operating the water dipper (0.06 cc dipper cup) via a toggle switch whenever the rat approached the array. The rats then had to learn how to find the S+ stimulus position, and, upon finding it, poking at the stimulus with their nose. The choice was recorded via an infrared touch screen (Carroll touch, USA) placed over the monitor face and if correct, it was rewarded with a drop of water. Experiment control was carried out with an MS-DOS based personal computer [27]. After initial training, the rats were tested in daily training sessions consisting of 40 trials each. No response was recorded for 4 s after stimulus onset, thus allowing the rat to search the stimulus, but stimulus presentation was terminated by the rat's response, which was followed by a 5 s water dipper activation and a 5 s inter-trial interval. For this and the remaining training and testing sessions, nose pokes to lo-

cations with an incorrect (non-reinforced) stimulus initiated a correction procedure. The trial in that case ended without a reinforcer, an error time-out (10 s) was scheduled, and the trial was repeated with the grating in the same place. Rats were trained daily in this manner until performance stabilized at above 80 % accuracy over three consecutive sessions (note that chance level with 6 stimuli is 16.7 %).

As soon as shaping performance was stable, the distractor luminance was progressively increased until it became equal to the grating mean luminance (10 steps). This testing schedule was continued until performance again stabilized at above 80 % accuracy over three consecutive sessions for the grating mean luminance step. Then, rats learned the contrast discrimination test by itself.

Contrast threshold analysis: Testing sessions consisted of a simple non-algorithmic adaptive procedure. For only one spatial frequency 0.14 cyc/deg, which corresponds to the spatial sensitivity peak, grating contrast was systematically reduced (descending series) until the rat performance fell below chance (16.7 %). Only after this training procedure was completed and stabilized, RGCs were labeled and the optic nerves were crushed and post-surgery testing commenced.

Behavioral performance was analyzed by two parameters: (1) as percentage of correct choices at a given contrast (% CC), and (2) as contrast performance (inverse of contrast threshold, CP). The contrast threshold is a particularly useful measure, as it is the point of inflection of a psychometric function which relates some physical measure of stimulus intensity (e.g. contrast) to some performance measure of detection (e.g. percentage of correct choices). It is the minimum contrast (MC) the rat requires to detect a particular grating. We used the maximum likelihood fitting program, MLPFTT, available with the ML-TEST package designed by Harvey [21], to fit, individually for each rat, a logistic function to the total binary response data and to obtain this contrast threshold measure.

Daily data were pooled into 5-day blocks to reduce the variance that results from daily variations in behavioral performance. "Days after surgery", as displayed in the figures, refers always to the respective mid point of each 5-day block.

2.3. Surgery

After rats had learned to perform the contrast discrimination test, retinal ganglion cells were labeled retrogradely under anesthesia (Ketamine 50 mg/kg – Rompun 10 mg/kg, i.p., Parke-Davis, Berlin/Bayer, Leverkusen, Germany) by injecting 2 μ l of fluorescent orange latex beads (orange FluoSpheres, undiluted, Molecular Probes, Leiden, the Netherlands) into the right superior colliculus (coordinates: ant-post 6.5 mm, lateral 1.4 mm, 3.0/3.5 mm below dura).

Ten days later, a bilateral optic nerve crush was carried out as described previously [9,46] under chloralhydrate anesthesia (7 %, 6 ml/kg, i.p.). The optic nerve was approached from the orbit by a lateral canthotomy under the guidance of a surgical microscope. The optic nerve was ex-

posed by blunt dissection, leaving both retinal blood supply and dura intact. The nerve was then crushed with a calibrated forceps at a distance of 2–3 mm from the eye for a duration of 30 s [46]. After completion of the crush, the canthotomy was sutured and an antibiotic eye ointment was topically applied to prevent inflammation (Aureomycin[®] Lederle Arzneimittel GmbH, Wolfratshausen, Germany).

Rats were randomly assigned to one of five groups. In sham rats ($n = 5$), surgery was carried out but the optic nerves were left intact. In a further three groups, ONC was applied at different severities: in mild crush ($n = 15$) the jaws of the forceps were separated by 0.2 mm in "rest-position", 0.1 mm in moderate crush ($n = 15$) and just touching each other in severe crush ($n = 10$). In the last group ($n = 4$), an optic nerve axotomy was performed after RGC labeling, but contrast discrimination performance was not tested.

2.4. Anatomical studies of retinal ganglion cells *in vivo*

In vivo confocal neuroimaging, ICON [43], was carried out five days after the injection of the fluorescent marker in all rats and again on the day prior to ONC. Every 5 days after ONC, RGCs were imaged with the ICON. On days of ICON imaging, no behavioral testing was carried out.

ICON sessions: ICON-imaging was carried out as previously described [43]. Briefly, in anaesthetized rats (same procedure as described above) the eye was treated with Neosynephrine-POS 5 % (Ursapharm, Saarbrücken, Germany) to relax the iris, and Vidisic optical gel (M. Pharma, Berlin, Germany) was applied as an immersion medium for the contact lens and to prevent drying of the cornea. The rats were then positioned underneath a standard confocal laser scanning microscope (Odyssey-XL, Noran Instruments GmbH, Bruchsaal, Germany) with a large probe space and long working distance objective lens. The left eye, containing the fluorescence labeled RGCs, was positioned directly underneath the objective lens, and to adjust the path of the laser rays to the rat eye, a Hruby-style-160 dioptin plano-concave contact lens (KPC-013, Newport GmbH, Darmstadt, Germany) was placed directly onto the surface of the cornea.

To measure cell size *in vivo*, the laser was focused (4 \times magnification objective lens) on a 0.08 mm² region located at approximately 30° eccentricity (which is about 2.0 mm lateral to the optic disc). The best images were obtained by using a scanning time of 400 ns (15 pics/s) and an average of 32 scanning acquisitions.

Soma size measurements: To follow cell size changes, we determined, as previously described [40] a well-defined area which contained a sufficient number of cells and which could easily be relocated at repeated time points using blood vessel morphology as landmark criteria.

To quantify cell sizes, an image analysis system (Q-500MC system, Leica, Bensheim, Germany) was used, and the limits between the fluorescent cells and the background were detected automatically by a gray scaling method. As we observed the retina *in vivo* through the living rat eye, the confocal microscope resolution was reduced to

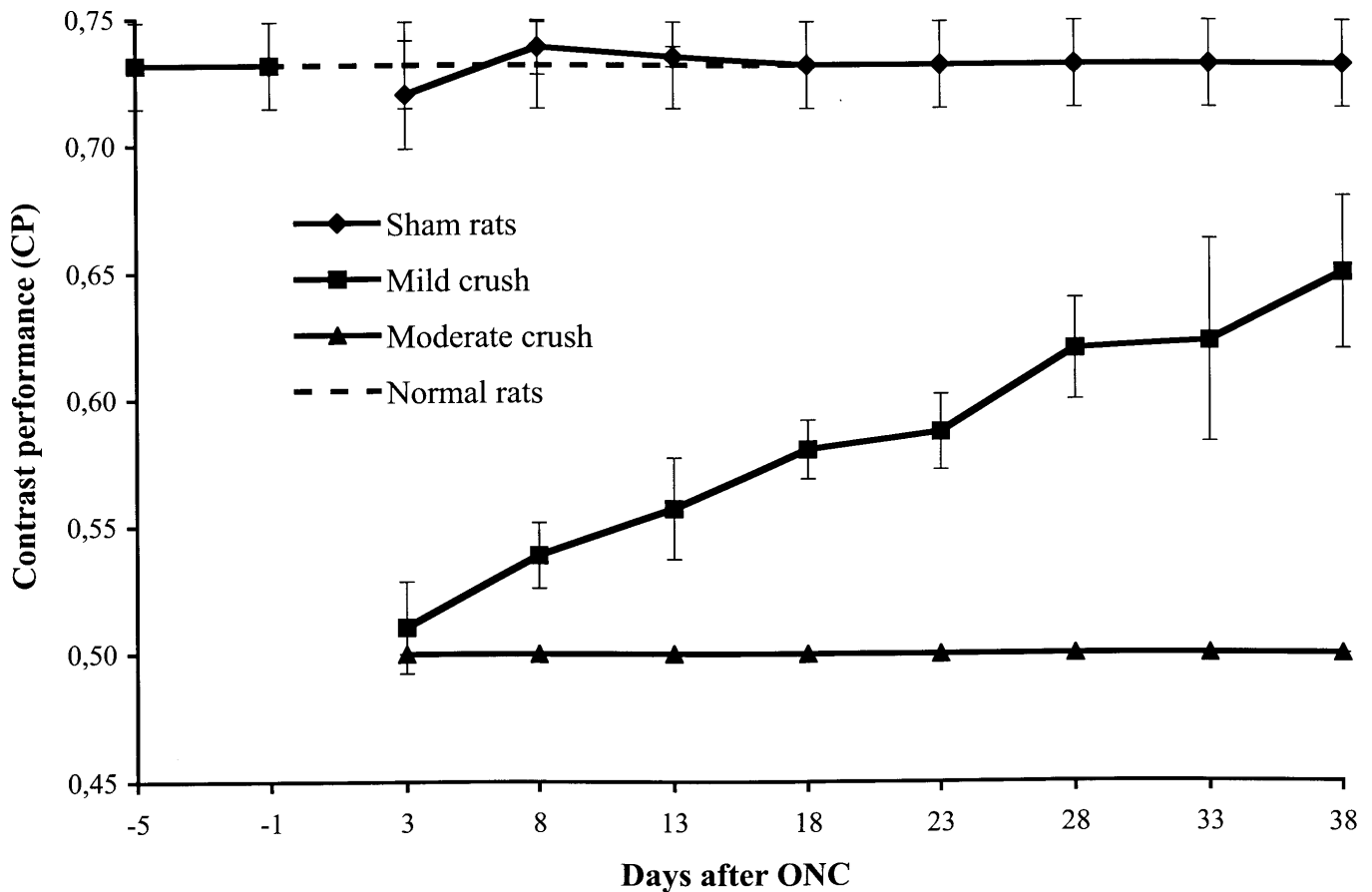


Fig. 1. Contrast discrimination performance (one-way ANOVA in conjunction with a post hoc Scheffe *t*-test, significance level set at $p < 0.01$). Sham rats: $CP = 0.73 \pm 0.02$, $MC = 23\%$, mild ONC: at P3 $CP = 0.5 \pm 0.02$, $MC = 91\%$, at P38 $CP = 0.65 \pm 0.1$, $MC = 34\%$, moderate ONC: CP at the inferior limit of the test, severe ONC: it was impossible to determine a CP in these animals.

avoiding false positives and thus limit the counting just to the RGC soma and not to other staining artifacts. The cell diameter was then quantified for each cell by the following procedure: cell soma diameters were drawn manually at five different angles in each cell on the monitor of the imaging system. The distance was then measured and averaged automatically to determine the mean cell diameter as a measure of cell soma size. As the rat head was not in the exact same position every time, there was the possibility that magnification artifacts would produce erroneous cell size estimates due to the variable focus levels. To be able to compare RGC diameter at different time points, we have therefore calculated a focus correction coefficient by comparing repeated images of the blood vessel diameter at different time points.

We then compared the size of the same cell over time. The exact fate of each individual cell was followed over time to differentiate between those RGCs which eventually died and those which survived. As a decrease in signal intensity can occur due to a modification of the labeling localization or concentration (bleaching), individual cell labeling intensities were not considered as a criterion for cell sampling selection. Only cells which could be visualized before the injury and at all time points after the optic nerve crush were included as surviving RGCs in the final statistical analysis.

The dying RGCs were defined to be those which can be seen before the ONC and at P3 but which subsequently disappear from the image. Before the ONC, we observed, on average, between 25–30 cells in each rat. The total estimate in normal retinae based on these counts were about 95,000, which is within the known range. After the ONC, the cell number declined gradually such that at the last time point, only 8–9 cells/rat could be visualized and their diameter measured (approximately 30,927 RGCs).

2.5. Anatomical analyses in retinal whole mounts

To be able to compare the ICON results with standard histological procedures, at the end of the experiment rats were anaesthetized with chloralhydrate (0.8 g/kg i.p.) and perfused transcardially with 10 mM PBS. The left eye was quickly removed and immersed in 4% PFA in PBS. The retina was dissected out quickly in 10 mM PBS. Four radial cuts were made into the retina to facilitate tissue flattening.

With the help of the confocal microscope, four sampling areas were chosen in each retina according to the following, predetermined procedure: the retina was first divided in quadrants according to the 4 radial cuts. Thereafter, confocal images were taken at approximately 30° eccentricity of the retina in each quadrant, which roughly corresponds to the

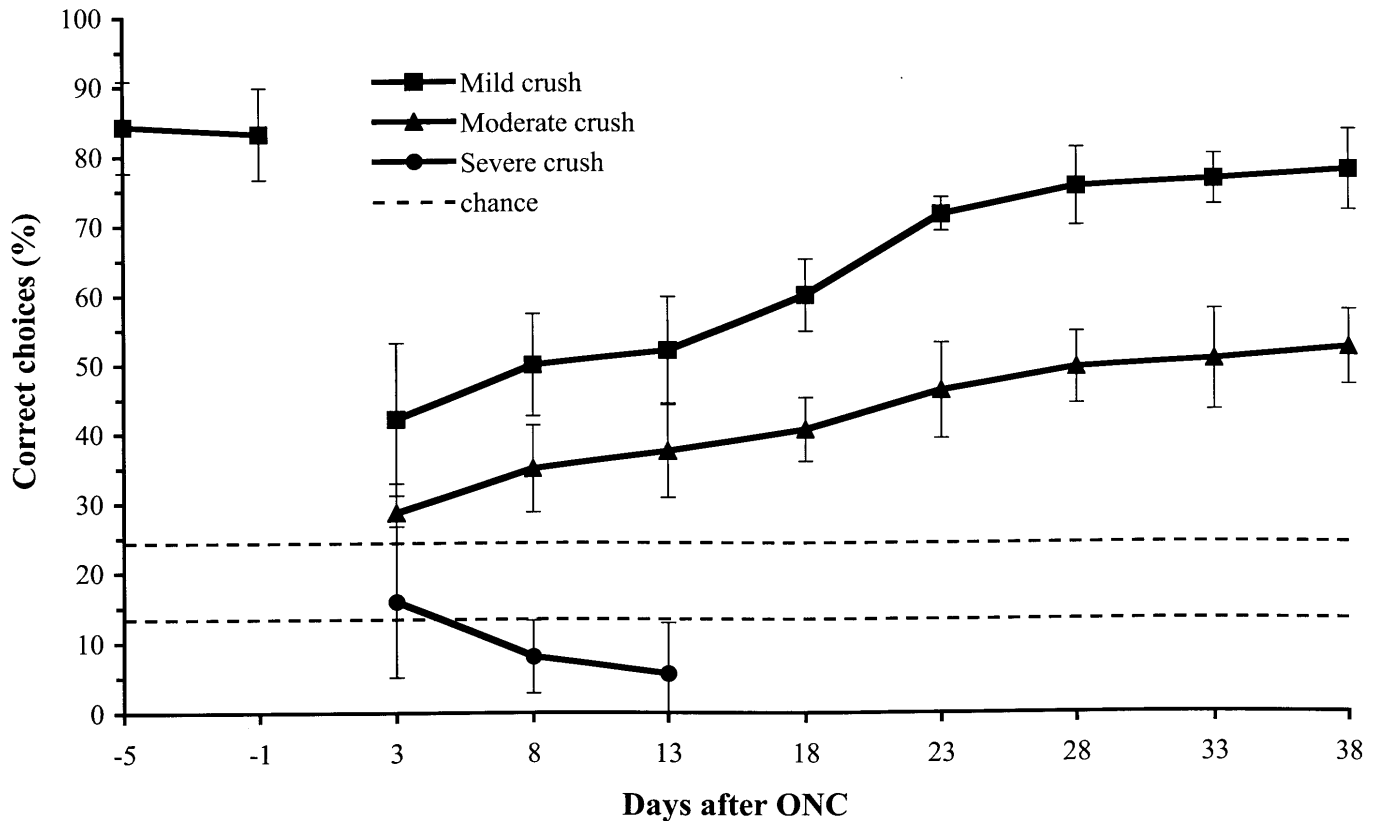


Fig. 2. **Discrimination performances at 96 % contrast.** (one-way ANOVA in conjunction with a post hoc Scheffe t-test, significance level set at $p < 0.01$). Mild ONC: at P3 %CC = 42.2 % \pm 11, at P38 %CC = 77.9 % \pm 6, moderate ONC: at P3 %CC = 28.6 % \pm 4, at P38 %CC = 52.4 % \pm 5, severe ONC: below chance (chance = 16.7 \pm 5 %).

area used for the *in vivo* imaging. Thereafter, cell density was quantified by the same image analysis used for the *in vivo* observations. A sampling area of 0.15 mm² was located in such a manner that it included, as accurately as possible, all cells which were also observed *in vivo*. Each area was counted twice. Objects smaller than 3 pixels in diameter were rejected by definition. Each cell was individually identified and manually counted. Cell density estimates in the retina were then calculated by taking the average of the four sampling regions.

To obtain a more accurate analysis of the RGC morphological changes, we calculated the relative cell size distribution. All cells were assigned to size-categories in steps of 2 μ m.

2.6. Statistical analyses

The behavioral tests and the anatomical analysis were done in blinded condition to avoid experimenter bias. The identity of the experimental condition of each rat was not known to the experimenter before data analysis.

RGC cell size measurements, calcium activity and contrast discrimination performance were analyzed by a one-way ANOVA used in conjunction with a post hoc Scheffé *t*-test to reveal statistical differences between groups. The significance level was set at $p < 0.01$.

To try to establish the mechanism of recovery, correlations (Pearson test) were analyzed between different morphological and visual parameters as a function of crush severity. This was carried out at 3 time points: at P3, P23 and P38 with the significance level set at $p < 0.05$. Any correlation coefficient of $r > 0.85$ was considered to be significant.

3. Results

3.1. Contrast discrimination

Prior to surgery, rats learned to discriminate contrast which required about 1 month of training, eventually reaching a contrast performance of 0.73 ± 0.02 ($n = 45$, $p < 0.01$, Fig. 1). The minimum contrast (MC), i.e. the lowest contrast level at which the rats were still able to respond to the stimuli above chance, was 23 %.

In the control rats, the surgery induced a temporary, but non-significant loss of contrast discrimination performance from which the rats recovered completely by P8 when they reached normal values ($CP = 0.74 \pm 0.01$).

Rats with bilateral ONC experienced a severe loss of contrast discrimination performance, the extent of which depended on crush severity. As shown in Fig. 1, in rats with mild ONC the contrast performance was 0.5 ± 0.02 ($p < 0.01$) a few days after the injury (P3). The rats could solve the visual

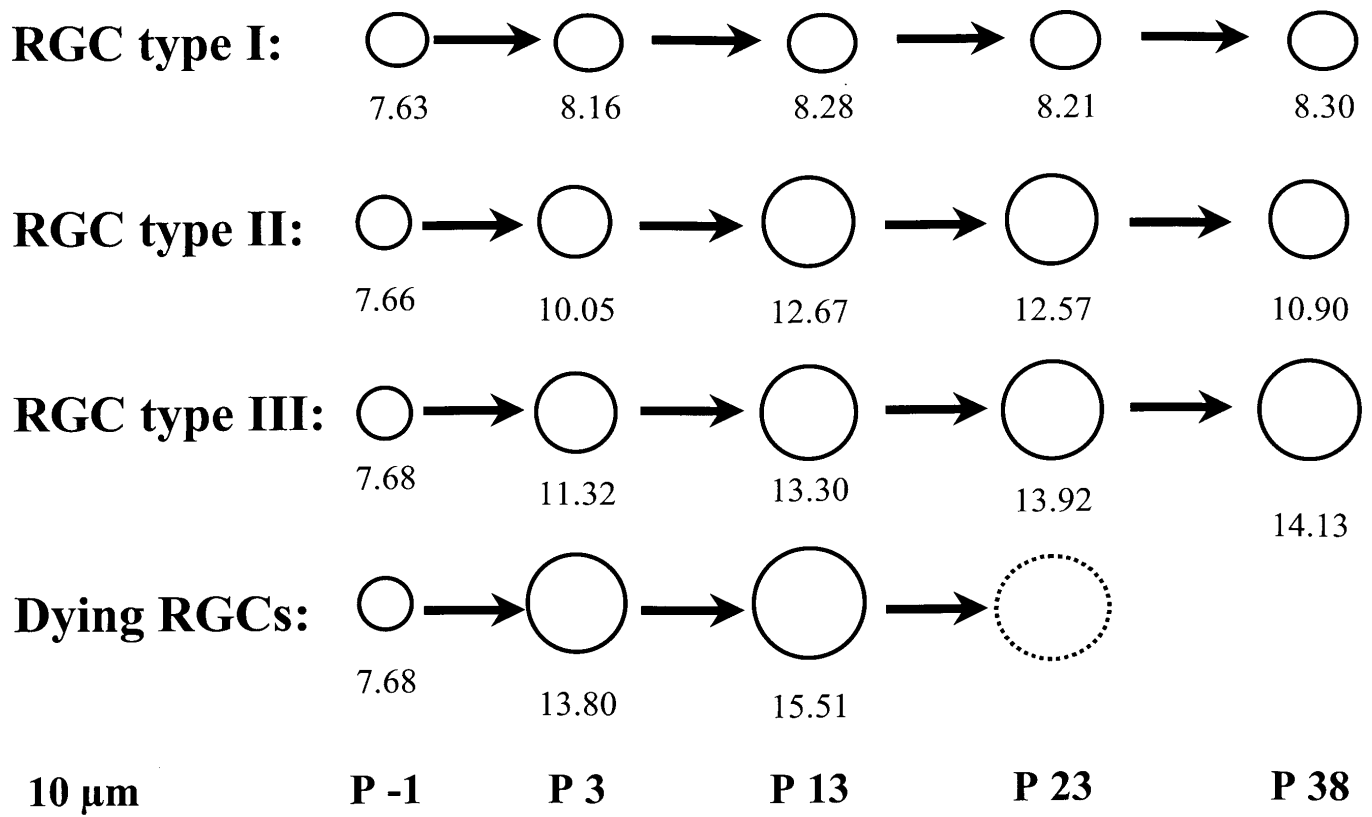


Fig. 3. **RGC diameter modifications.** (one-way ANOVA in conjunction with a post hoc Scheffé *t*-test, significance level set at $p < 0.01$). *RGC type I*: mild and moderate crush data have been pooled. These cells show no soma size increase, they comprise 44 % of the surviving RGCs after mild ONC (40 % after moderate ONC) and they are not found after a severe ONC or axotomy; *RGC type II*: soma size increase of 66 % over baseline (compared to sham operates) within first 10 days; thereafter, size stabilization until P23. From P28 until the end of the experiment, we observed a soma size decrease. At P38, soma size was found to be 31 % above baseline; this was observed in 56 % of the surviving RGCs after a mild ONC, but it was not found in the other groups. *RGC type III*: here, there is a soma size increase of 86 % over baseline until P38; this type comprises 60 % of the surviving RGCs after a moderate ONC. Such cells were not found in the other groups. *Dying RGCs*: all crush groups were pooled for this graph. We observed a soma size increase of 136 % over baseline until P13 with subsequent cell death. This was found in all crush groups. All cells belonged to this class after a severe ONC or axotomy.

task above chance only at the maximum contrast ($MC = 91\%$). Thereafter, the contrast discrimination progressively improved to reach 0.65 ± 0.1 ($MC = 34\%$, $p < 0.01$ compared to P3) during the last days of testing (P38).

In the moderate injury group, the rats tried to solve the task, but they were severely impaired in their contrast discrimination performance (CP at the lowest limit of the test). However, at the highest contrast level of 96 % (Fig. 2), these rats recovered somewhat, though clearly to a lesser extent, than their mild crush counterparts. At P3, the percentage of correct choices was only $28.6\% \pm 4$, which is close to chance level (17 %), but performance improved gradually thereafter until P38 ($\% CC = 52.4\% \pm 5$, $p < 0.01$ compare to P3 or to the severe crush). This performance was below that of the mild ONC rats at P3, which had a score of $42.2\% \pm 11$ at maximal contrast ($\% CC = 77.9\% \pm 5.8$ at P38, $p < 0.01$).

In the severe ONC group, it was not possible to determine a contrast threshold. Rats were unable to perform the task at all as most of them even did not poke their nose at the screen anymore. Those rats appeared completely blind. They were therefore sacrificed 15 days after ONC. In rats with severe injury, the percent of correct choice was below chance at all

time points, despite the highest contrast level (Fig. 2, $\% CC = 16\% \pm 10$ at P3, $5\% \pm 8$ at P13).

3.2. Retinal ganglion cell morphology as observed in vivo with ICON.

In control rats the average RGC diameter was found to be $7.6 \mu\text{m} \pm 0.1$, with no significant cell diameter changes over time. As expected, in all ONC groups, the pre-surgery RGC sizes were almost identical (Fig. 3). After ONC, however, ICON revealed that surviving RGCs experienced anatomical modifications, i.e. cell soma swelling which depended on the respective crush severity (see also [40]). Based on the extent and time-course of soma swelling we propose that there are four different types of RGCs after injury (Fig. 4):

RGC type I: these RGCs were presumably unaltered or had only slight changes in their soma size over time (Figs. 3, 4, no significant change, even when we compared P-1 with P38) and which could still be seen at P38 (average diameter of $8.3 \mu\text{m} \pm 0.5$). After mild ONC, these cells comprise about 44 % of the surviving cell population, (approximately 13,745 RGCs), and after moderate ONC 40 % (10,309 RGCs). After severe ONC or axotomy, no type I cells were observed in the retina.

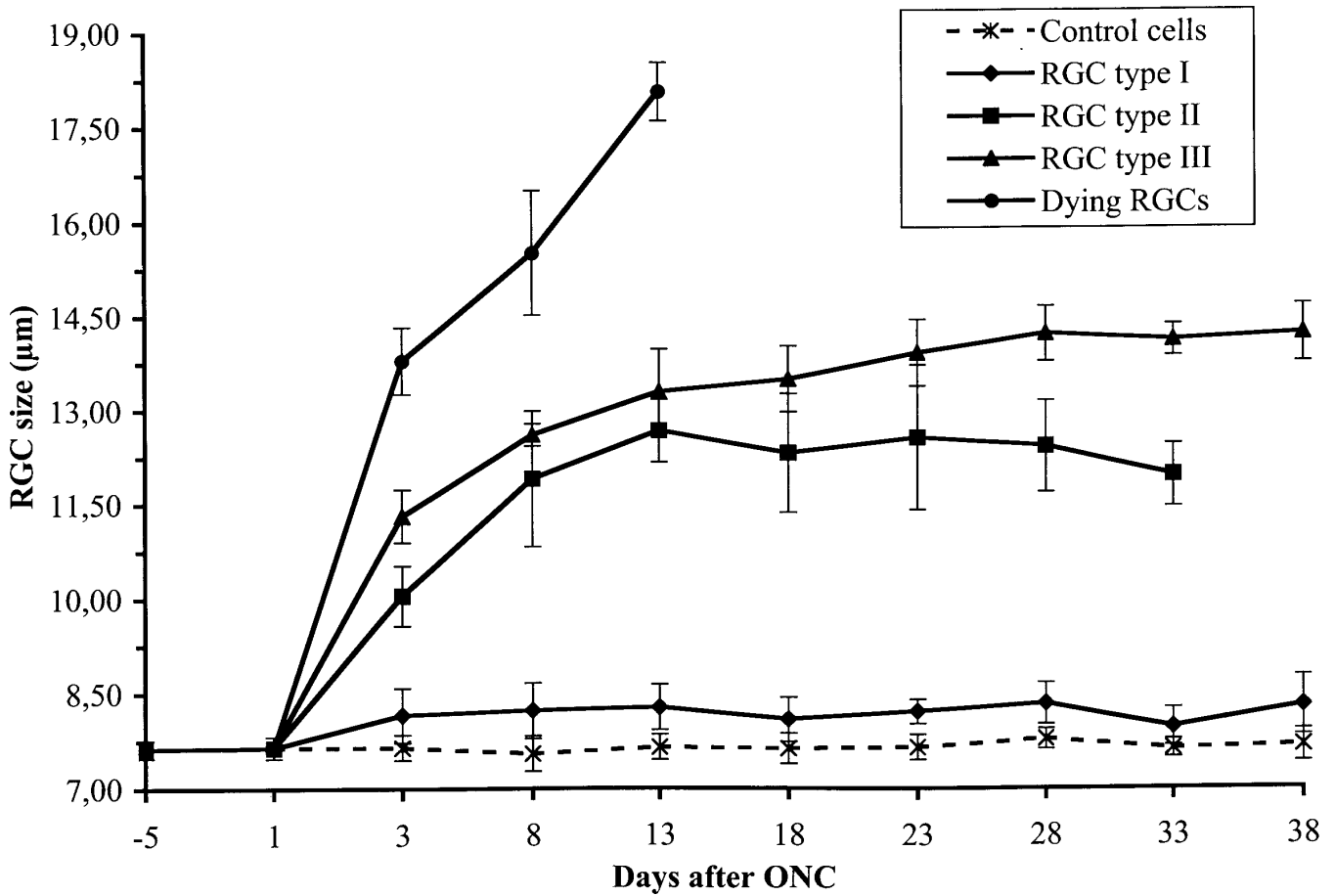


Fig. 4. Different RGC types found after ONC. RGC type I: normal surviving RGCs without soma size modification. RGC type II: surviving RGCs which undergo a transient, slow and moderate soma size increase. RGC type III: surviving RGCs which undergo a slow but continual and more pronounced soma size increase. Dying RGCs: RGCs which undergo a rapid and massive soma size increase and then die. The values are the mean diameter in µm; scale bar = 10 µm; P = days after ONC.

TABLE 1. Correlation between Behavioral and anatomical parameters (mean ± SE, one-way ANOVA in conjunction with a post hoc Scheffe t-test, significance level set at $p < 0.01$). RGC type I, RGC type II: and, RGC type III as defined in legend to Fig. 3. % of RGCs corresponds to the percentage of RGCs of one type that can be seen at the respective time point.

	Sham rats (n = 5)		Mild ONC (n = 15)				Moderate ONC (n = 15)			
	P3	P38	P3	P13	P23	P38	P3	P13	P23	P38
Behavior results										
CP	0.72 ± 0.02	0.73 ± 0.04	0.51 ± 0.02	0.56 ± 0.02	0.59 ± 0.02	0.65 ± 0.03	0.5	0.5	0.5	0.5
% CC (C = 96 %)	84.5 ± 2.9	85 ± 3.1	42.2 ± 11	52.1 ± 7.7	71.7 ± 2.4	77.9 ± 5.8	28.6 ± 4.4	37.5 ± 6.7	40.6 ± 4.6	52.4 ± 5.4
Diameter (µm)										
RGC type I	7.65 ± 0.2	7.65 ± 0.2	8.16 ± 0.4	8.25 ± 0.3	8.21 ± 0.2	8.26 ± 0.5	8.17 ± 0.2	8.28 ± 0.4	8.31 ± 0.2	8.30 ± 0.5
RGC type II	-	-	10.05 ± 0.5	12.67 ± 0.5	12.57 ± 1.2	11.0 ± 0.6	-	-	-	-
RGC type III	-	-	10.05 ± 0.5	12.67 ± 0.5	12.57 ± 1.2	11.0 ± 0.6	11.32 ± 0.4	13.3 ± 0.7	13.92 ± 0.5	14.23 ± 0.5
Dying RGCs	-	-	13.48 ± 0.5	17.08 ± 0.5	-	-	13.80 ± 0.5	18.02 ± 0.6	-	-
% of RGCs										
RGC type I	100	100	6.61 ± 2	17.64 ± 5	30.87 ± 7	44.1 ± 9	6.04 ± 3	16.12 ± 2	28.21 ± 1	40.3 ± 7
RGC type II	-	-	9.88 ± 3	26.36 ± 2	43.13 ± 8	65.9 ± 6	-	-	-	-
RGC type III	-	-	-	-	-	-	8.95 ± 5	23.88 ± 4	41.79 ± 6	59.7 ± 8
Dying RGCs	-	-	83.51 ± 6	56 ± 9	-	-	85.01 ± 12	60.0 ± 13	-	-

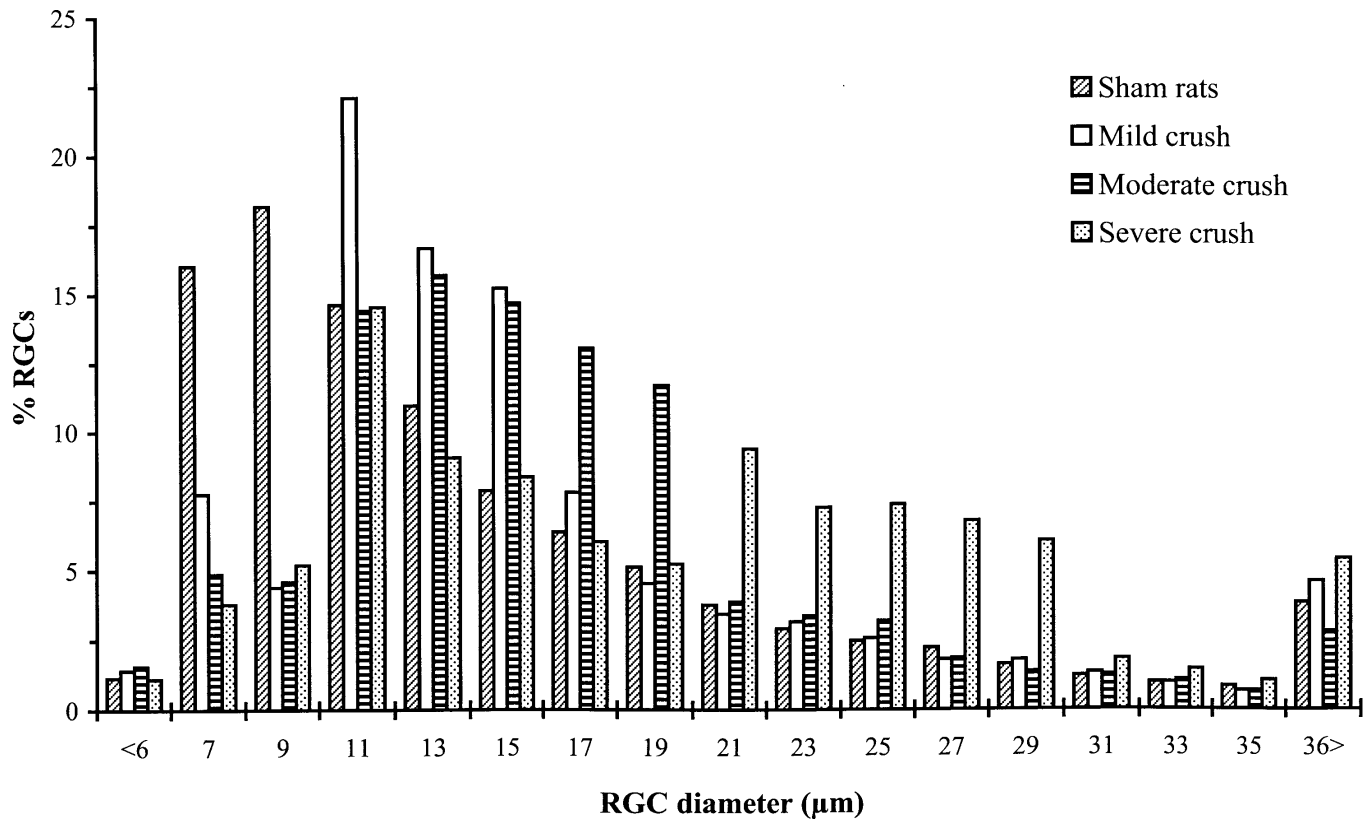


Fig. 5. RGC size distribution in retinal whole mounts. (one-way ANOVA in conjunction with a post hoc Scheffe *t*-test, significance level set at $p < 0.01$). Due to the soma size increases, the surviving RGC soma size showed a shift from small and medium size towards bigger ones. Sham rats: 49 % of the RGCs ranged from 6–12 μm (instead of 24–34 % for the same size categories in the other groups). Mild ONC: 53 % of the RGCs ranged from 10–16 μm (instead of 33 % for the same size categories in the sham rats). Moderate ONC: 55 % of the RGCs ranged from 12–20 μm (instead of 24 % for the same size categories in the sham rats). Severe ONC: 37 % of the RGCs ranged from 20–30 μm (instead of 13 % for the same size categories in the sham rats).

RGC type II: these RGCs undergo a transient slow and moderate soma size increase (Figs. 3, 4), and, comparable to type I RGCs, they could still be visualized on P38. As Table 1 shows, type II cells could only be found in rats with mild ONC, where they corresponded to 56 % of all surviving RGCs (about 17,182 RGCs). These RGCs type II experienced a gradual and moderate soma swelling to 66 % over baseline (baseline control value = 100 %, $p < 0.01$) during the first 15 days after ONC (mean diameter $12.7 \mu\text{m} \pm 0.5$ at P13, $p < 0.01$). Thereafter, at P23, the cell size was stabilized at 64 % over baseline (mean diameter: $12.6 \mu\text{m} \pm 1.2$, $p < 0.01$). From P28 until the end of the experiment, the cell size then gradually declined again (mean diameter $11.0 \mu\text{m} \pm 0.6$ at P38) in a process of morphological recovery.

This corresponds to our previous observations of cells at P75, which had shrunken compared to the time of maximum cell expansion [40]. Yet (at P38), the cell diameters remained significantly elevated at about 31 % over baseline (mean diameter $10 \mu\text{m} \pm 0.2$).

RGC type III: these RGCs undergo a slow but continual and more pronounced soma size increase (Figs. 3, 4) which, unlike type II cells, did not stabilize at P13. Rather, type III cells gradually and continually increased their cell body size for the entire 40 days following the injury (mean diameter

$14.2 \mu\text{m} \pm 0.6$ i.e. 86 % over baseline, $p < 0.01$), without subsequent recovery. Although type III cells could also still be observed at P38, their long-term fate is not known. We only observed type III cells in rats with moderate ONC (Table 1), where they comprised about 60 % of all surviving RGCs (20,618 RGCs).

Dying RGCs: as previously reported, these RGCs undergo a massive and rapid soma size increase (136 % above baseline, mean diameter $18.1 \mu\text{m} \pm 0.5$, $p < 0.01$ at P13) and then disappear from the image at P13 or thereafter (Figs. 3, 4), presumably having died [40]. As a consequence, we could not follow a sufficient number of RGCs over time to describe any reliable cell modifications at later time points.

Dying cells are found in all ONC groups with no statistical difference among these groups or after axotomy ($p > 0.01$). Thus, there appears to be a highly vulnerable group of RGCs, which are destined to die, no matter how mild the injury, representing about 70 % of the entire RGCs population in rats with mild and moderate crush (the total number is about 63,571). After severe ONC or axotomy, all cells belong to this category.

It is obvious from figures 3 and 4 that the time course and the extent of cell swelling are distinctly different between

TABLE 2. Correlation coefficients (r) between visual performance and anatomical parameters as a function of crush severity. As it is not possible to obtain a contrast threshold after the moderate ONC, we used % CC at 96 % contrast (see legend to Fig. 2). The behavioral parameter used in mild crush rats (contrast performance) is therefore different from that used for moderately injured animals (% correct choice at 96 % contrast). As a consequence, the correlation analysis was performed for both groups separately (Pearson test with a significant level set at $p < 0.05$, coefficient > 0.85 was considered as significance, $n = 25$). For cell type definition see legend to Fig. 3. Number of RGCs (%) is the percentage of RGCs of one type that can be seen at the respective time point.

	Contrast performance		
	P3	P23	P38
<i>Diameter</i>			
RGC type I	0.63	0.28	0.11
RGC type II	0.56	0.88	0.96
RGC type III	0.42	0.80	0.98
Dying RGCs	-0.94	-0.11	-0.25
<i>% RGCs</i>			
RGC type I	0.85	0.59	0.42
RGC type II	0.26	0.85	0.94
RGC type III	0.35	0.65	0.95
Dying RGCs	-0.90	-0.55	-0.72

those cells which are destined to live and those which are destined to die, confirming our previous report [40]. At P3, most of the dying retinal ganglion cells had already undergone a dramatic size increase to 80 % over baseline ($p < 0.01$), instead of 31 % or 48 % found in the mild or moderate crush respectively, and their size increased until death.

3.3. Retinal ganglion cell density as measured in whole mounts

To obtain a cell number estimate which was independent of the ICON procedure, retinal whole mounts were prepared, and RGCs were imaged with the standard confocal laser scanning microscope set-up after the animals had been sacrificed. The number of RGCs was significantly reduced after injury for all injured groups. There were no significant differences between the different crush severities, which is essentially identical to the *in vivo* observation. Only $33\% \pm 5$ (approximately 31.185 RGCs) of the RGCs survived in the mild crush rats ($30\% \pm 5$ and $30\% \pm 5.5$ in the moderate and severe ONC groups respectively, i.e. about 28.350 RGCs, $p > 0.01$) which confirms the values obtained with the ICON-technique.

Note that although no RGC could be found after severe crush or axotomy with ICON, the retina whole mounts did contain surviving retinal ganglion cells with some fluorescence, but the fluorescence intensity was apparently below the detection level of the ICON. As a consequence, our inability to observe RGCs with ICON after P13 in the severe crush group does not imply that no RGCs had survived at all. It rather demonstrates that there are no longer any cells with a sufficiently brilliant fluorescence to be visible with ICON. Despite this technical limitation, loss of fluorescence in

ICON is a reliable indicator of cell death for the large majority of the cells. Secondly, we compared the retina whole mount of rats sacrificed at P40 (mild and moderate crush) with rats sacrificed at P15 (severe crush). In the case of the severe crush, not all dying RGCs had been eliminated, but 40 days after severe ONC there was a dramatically reduced RGC density.

Note, however, because the RGCs were labeled prior to ONC, the current protocol did not differentiate between axotomized cells and those cells which remained connected with their brain target. Only RGCs remaining connected with their brain target are expected to contribute to visual functions. At least in the mild ONC situation, that number is in the order of 10–20 % of the entire RGC population [46,45].

Due to the soma swelling we noted with ICON, the surviving RGCs showed an altered size distribution in the retinal whole mount: there was a shift from small and medium sized cells towards bigger ones (Fig. 5). In sham rats, 49 % of RGCs had a soma size ranging from 6 to 12 μm (instead of 24–34 % of RGCs for the same size categories in the other groups). After mild ONC, the soma size categories from 10 to 16 μm contained most cells: 54 % of all surviving RGCs. In control rats, this size class only contained 33 % ($p < 0.01$). After moderate ONC, the 12 to 20 μm categories contained most cells, i.e. 55 % of all surviving RGCs compared to 24 % in uninjured controls ($p < 0.01$). In the severe crush group, the size categories with most of the RGCs (37 %) were between 20–30 μm (control: 13 %, $p < 0.01$).

3.4. Correlation of morphology and behavior

To gain a better understanding of the relationship between morphological and behavioral parameters, we conducted a detailed correlation analysis. Particularly in view of the fact that ICON permits the simultaneous assessment of cell size changes over time and assessment of behavioral performance (for further details of the parameters, see Table 1), we reasoned that a morphological parameter may be found which correlates with behavioral outcome. We calculated correlation coefficients (r) between contrast performance (for the mild ONC) or percent of correct choice at 96 % contrast (for the moderate ONC), and the morphological measures of cell number and cell size. The results of these correlation analyses are displayed as a function of crush severity in Table 2.

Cell diameter: The diameter of RGC type I correlated with $r = 0.63$ or 0.73 (non-significant, though) with parameters of visual functions early (P3) after the injury and this correlation vanished thereafter. The diameter of RGC type II did not correlate early on, but correlated very highly (up to $r = 0.96$ or 0.98 , respectively, $p < 0.05$) at later periods of time after the ONC, i.e. at P23 and P38. As Table 2 shows, the correlation improved over time both in the mild and in the moderate crush group. Regarding the RGC type III, which were only found in the moderate injury group, the correlation between visual performance and the diameter became significant only at P38 ($r = 0.98$, $p < 0.05$). The diameter of dying RGCs and the visual scores are negatively correlated immediately after the injury

($r = -0.94$, $P < 0.05$) but not later on. Thus, compensatory cell diameter swelling highly correlates with recovery of vision.

Cell numbers: We found a good correlation immediately after ONC (P3) between visual performance and the number of RGC type I, expressed by the percentage of RGCs that can be seen at each time point ($r = 0.85$, $p < 0.05$). Over time, this correlation disappeared. With regard to the RGC type II population a correlation developed by P23 of $r = 0.85$ or 0.87 ($p < 0.05$) in the mild and moderate group, respectively, and $r = 0.94/0.97$ ($p < 0.05$) at P38, respectively, between visual performance and the cell number. Cell number is again expressed as the percentage of RGCs that can be seen at each time point ($r = 0.85$, $p < 0.05$). As with the diameter change, the correlation thus improved over time. The correlation between visual performance of the moderate group and their RGC type III population became significant only at P38 ($r = 0.95$, $p < 0.05$). The correlation of the dying RGC population and the visual scores was negative immediately after the injury ($r = -0.90$, $P < 0.05$), vanishing over time.

Thus, the correlation analysis shows that type I RGCs are apparently important for the visual performance at P3 and the more dying cells, the worst the vision. As time progresses, the compensatory swelling of the surviving cells (both in terms of diameter increases and number of cells showing such increases) becomes more and more important for performance, being the prominent factor determining outcome. Thus, cells which do not change their diameter determine vision immediately after the injury, while cells with compensatory some swelling (type II or type III cells) provide the structural basis for recovery of vision.

4. Discussion

To help delineate the neurobiological mechanisms of recovery of vision [45], repeated *in vivo* imaging of the retinal ganglion cells with ICON was combined, in the same rat, with the assessment of visually guided behavior following ONC. In particular we were interested in the correlation of previously described cell size modifications [40] and contrast discrimination performance. In agreement with previous studies [45], rats with mild ONC recovered some of their performance (though not to normal levels), the extent of which depended on lesion severity.

Specifically, the number of RGCs without compensatory soma size increases (type I cells) correlates highly with visual performance early after the lesion. This suggests that type I cells are unaffected by the neurotrauma and that their function is to maintain the sparse, residual visual functions immediately after injury, well before recovery takes place. In contrast, the number of dying cells correlates highly and negatively with visual performance.

The most important finding of the present experiment is the discovery of very high correlations ($r = 0.96$) between compensatory cell body swelling, expressed in terms of both the extent of diameter increases and number of Type II and III

RGCs, and recovery of vision. These RGC type II and type III cells experience a slow and moderate soma size increase which is distinctly different, in both time course and extent, from cell death-related soma swelling, confirming previous reports [40]. The 2–3 week time course of this “compensatory”, moderate soma size increase is strikingly similar to physiological parameters of recovery of vision [47,45]. The difference between type II cells and type III cells is that the former partially recover back towards normal size a few weeks after injury whereas the latter do not [40]. It is apparent from these observations that compensatory cell size increases may play an important role in recovery and plasticity.

Others have also noted cell size increases that appeared to relate to compensation or cell survival. Chow and Steward [5], who conduct monocular deprivation experiments with kittens, noted many neurons in the lateral geniculate nucleus of the deprived eye which, when later exposed to visual stimulation, showed enlarged soma diameters even above control levels. Also, Moore and Thanos [36] noted RGC size increases after both axotomy and ONC which appeared to relate to cell survival. Despite these reports, however, we are not aware of such clear-cut demonstrations that cell size increases are indeed adaptive for the injured brain or that they are behaviorally meaningful. Therefore, the findings of the present study are the first demonstration of the role of compensatory cell soma increases in the process of recovery of function.

Compensatory cell swelling as a substrate for recovery of vision: Based on these findings we now propose that the retrograde reaction of compensatory cell body swelling is of adaptive significance for recovery of function. Because the correlations between morphological/cellular alterations and behavioral outcome (recovery) are so high, which has not been reported before, it may be concluded that compensatory soma size increases are an important neurobiological substrate of recovery of function in general and recovery of vision in particular. Though correlations do not inform us about causality, because the morphological changes of compensatory soma swelling appear first and the behavioral improvements later, the relationship is likely to be causal.

The visual system is a particularly suitable model to now address questions of post-lesion plasticity and repair in animals [2,6,7,11,16,17,37,55] and humans [23,25,26,28,53]. Because visual system structures in the brain receive their only visual input from the retina, it is not conceivable that vision is taken over by non-visual structures. Any recovery must therefore be mediated by structures of the partially injured system itself or up-stream areas. In the “minimal residual structure hypothesis” [41] one of us has already argued that as long as the lesion is diffuse and the amount of injury does not exceed a certain critical size, recovery of function occurs [4,1,44]. While a certain minimum number of cells is required for any structure to recover from injury, there is no clear-cut correlation between the number of surviving, retrograde cell bodies (without also considering their connectivity and soma sizes) and functional outcome [42,45,46]. Just counting retrogradely surviving cell bodies does not only fail

to predict behavioral recovery [42,45,46], but in some instances fewer cells may, in fact, be associated with better functional recovery [48]. In the present study the number of surviving cell bodies was also not significantly different among the three different lesion groups even though their visual performance are markedly different. Thus, it is not the number of surviving cell bodies which matters for function, but it is rather the compensatory cellular reaction to the trauma, i.e. the extent of compensatory soma swelling that predicts behavior and its associated events.

That a relatively small number of cells is apparently sufficient for some visual functions has been observed before. Lashley [30], for example, has already shown that with only 1/5 of the cells in the lateral geniculate nucleus of the thalamus, rats are able to discriminate visual forms. Similarly, in humans with residual visual capacity small remnants of tissue are apparently sufficient for blindsight to occur [12,35,54]. Also, Cowey et al. [8] suggest that, in rats operated neonatally, a reduced acuity is a direct consequence of the loss of RGCs. However, when the rats are operated at different ages later in their life, their acuity is indistinguishable despite the large difference in the extent of ganglion cell loss [32]. Another relevant observation was made by Heywood et al. [22] who found that despite reducing the number of ganglion cells by about 70 %, contrast sensitivity remained normal as measured electrophysiologically in striate cortex. These reports thus confirm our conclusion that it is not the number of surviving cells which determine whether vision recovers or not, but it is the manner how surviving cells react to the neurotrauma.

Biological basis for cell soma swelling: The question arises how the compensatory soma swelling occurs and if it is a primary plasticity event or a process secondary to other alterations. We think that the compensatory swelling itself is probably not the crucial mechanism underlying recovery of visual functions but a coincidental event secondary to changes inside the cell such as alterations in dendritic or terminal fields and changes inside the damaged axons themselves. While this needs further experimentation, reports by others may guide us to formulate hypotheses. For example, injury to the optic nerve induces a massive increase in RNA synthesis followed by an increase in protein synthesis [20,34]. Conceivably, surviving cells may increase their soma size because their axonal injury places a metabolic demand on their cell body (such as production of cytoskeletal proteins) which, in turn, increases the cell soma size in response to this synthesis. We have most recently obtained evidence that following optic nerve crush axons with internal damage are able to repair their damaged neurofilaments and thus re-establish their axonal transport (Hanke and Sabel, unpublished observations).

The increased soma size may also reflect changes in the metabolic activity of cells required to maintain an extended axon tree which is formed by collateral axon sprouting induction as demonstrated in the visual system [10] or the hippocampus after injury. In the hippocampus, similar soma size increases have been reported [50].

Soma size increases are also frequently reported in the regeneration literature. Particularly those surviving RGCs with large somata are predominantly able to regenerate their axons [24,39], and cell body sizes of regenerating RGCs increase for several weeks after peripheral nerve transplantation [31,51,52]. Thus, cell soma swelling may be an expression of a regenerative response, the nature of which is currently being studied in our laboratory (possibly intrinsic axon repair). Because recovery of vision occurs rather fast (within a couple of weeks) but long-distance axon regeneration more slowly (a few months), compensatory soma size increases are unrelated to axon regeneration. Indeed, the recovery of bidirectional axon transport and the restoration of heavy neurofilaments in surviving axons with internal damage may be related to the compensatory swelling phenomenon (Hanke and Sabel, unpublished).

The time course of the compensatory swelling is a steady, linear incline reaching a plateau at 15 days [40] or 28 days (this study). This parallels the improvement of visual function seen in this and all other previously published studies [45]. As we have seen in our previous study [40], but not as pronounced in the present experiment, after about 1 month the cell swelling itself recovers somewhat and swollen RGCs type II, but not type III, partially shrink back towards normal levels. But because this occurs at a time when recovery of vision has already reached its maximum (recovery usually peaks at 14–21 days), recovery from soma swelling is probably not the cause but is the consequence of a cellular repair process. It is conceivable that axons which are internally damaged, but not axotomized, play a special role in recovery of function [18,44], and first evidence for this has been obtained in our laboratory (see above).

In summary, we found a very high correlation between retrograde RGC soma swelling and recovery of visual performance. In fact, by simply measuring cell soma sizes it is possible to predict with high accuracy, whether or not an individual rat will recover its visual functions. Because of the parallel time course of compensatory swelling and recovery, the relationship between both is not just coincidental. Rather, moderate soma swelling is the cause, and not the effect, of recovery and it may therefore be a prominent mechanism underlying nervous tissue repair. Because cells experiencing such a slow and moderate soma size increase play a special role in the recovery process, we now propose to term these cells “compensatory neurons“.

Acknowledgements

Supported by grants from the Deutsche Forschungsgemeinschaft (DFG), by the State of Sachsen-Anhalt and by the Ministry of Education and Research (BMBF, Neurotraumaverbund Magdeburg/Berlin, TP A2). We thank Kerstin Hahn and Steffi Matzke for administrative assistance and Uta Werner for technical help with the experiments.

References

- [1] Basso, D.M., Beattie, M.S. and Bresnahan, J.C. Graded histological and locomotor out-comes after spinal cord contusion using NYU weight-drop device versus transection. *Exp. Neurol.* **139** (1996) 244–256.
- [2] Berardi, N., Lodovichi, M., Caleo, M., Pizzorusso, T. and Maffei, L. Role of neurotrophins in neural plasticity: what we learn from the visual cortex. *Restor. Neurol. Neurosci.* **15** (1999) 125–136.
- [3] Bien, A., Seidenbecher, C.I., Böckers, T.M., Sabel, B.A. and Kreutz, M.R. Apoptotic versus necrotic characteristics of retinal ganglion cell death after partial optic nerve injury. *J. Neurotrauma* **16** (1999) 153–163.
- [4] Castaneda, E., Wishaw, I.Q. and Robinson, T.E. Changes in striatal dopamine neurotransmission assessed with microdialysis following recovery from a bilateral 6-OHDA lesion: variations as a function of lesion size. *J. Neurosci.* **10** (1990) 847–1854.
- [5] Chow, K.L. and Stewart, D.L. Reversal of structural and functional effects of long-term visual deprivation in cats. *Exp. Neurol.* **34** (1972) 409–433.
- [6] Chino, Y.M. Adult plasticity in the visual system. *Can. J. Physiol. Pharmacol.* **73** (1995) 1323–1338.
- [7] Chino, M.Y. The role of visual experience in the cortical topographic map reorganization following retinal lesions. *Restor. Neurol. Neurosci.* **15** (1999) 165–176.
- [8] Cowey, A., Henken, D.B. and Perry, V.J. Effect on visual acuity of neonatal or adult tectal ablation in cats. *Exp. Brain Res.* **48** (1982) 149–152.
- [9] Duvdevani, R., Rosner, M., Belkin, M., Sautter, J., Sabel, B.A. and Schwartz, M. Graded crush of the rat optic nerve as a brain injury model: combining electrophysiological and behavioral outcome. *Restor. Neurol. Neurosci.* **2** (1990) 31–38.
- [10] Eysel, U. and Peichl, L. Regenerative capacity of retinal axons in the cat, rabbit and Guinea pig. *Exp. Neurol.* **88** (1985) 757–766.
- [11] Eysel, U.T., Schweigart, G., Mittmann, T., Eyding, D., Arckens, L., Qu, Y., Vandesande, F. and Orban, G. Reorganization in the visual cortex after retinal and cortical damage. *Restor. Neurol. Neurosci.* **15** (1999) 153–164.
- [12] Fendrich, R., Wessinger, C.M. and Gazzaniga, M.S. Residual vision in a scotoma: implications for blindsight. *Science* **258** (1992) 1489–1491.
- [13] Finger, S. and Stein, D.G. *Brain damage and recovery*. New York: Plenum, 1982.
- [14] Flohr, A.P. *Post-lesion neural plasticity*. Berlin: Springer-Verlag, 1988.
- [15] Freund, H.J., Sabel, B.A. and Witte, O. *Brain plasticity*. New York: Lippicott Raven Press, 1997.
- [16] Frost, D. Functional organization of surgically created visual circuits. *Restor. Neurol. Neurosci.* **15** (1999) 107–113.
- [17] Galuske, A.W., Kim, D.-S. and Singer, W. The role of neurotrophins in developmental cortical plasticity. *Restor. Neurol. Neurosci.* **15** (1999) 115–124.
- [18] Gennarelli, T.A., Adams, J.H. and Graham, D.I. Diffuse axonal injury: A new conceptual approach to an old problem. In A. Baethmann, S. Go and A. Unterberg A (Eds.). *Mechanisms of secondary brain damage*. Plenum editor, New York, 1986, pp. 15–28.
- [19] Gennarelli, T.A., Thibault, L.E., Tipperman, R., Tomei, G., Sergot, R. and Brown, M. Axonal injury in the optic nerve: a model simulating diffuse axonal injury in the brain. *J. Neurosurg.* **71** (1989) 244–253.
- [20] Grafstein, B. and McQuarrie, I.G. Role of the nerve cell body in axonal regeneration. In C.W. Cotman (Ed.). *Neuronal Plasticity*, Raven Press, New York, 1978, pp. 155–195.
- [21] Harvey, L.O. Jr. Efficient estimation of sensory thresholds. *Behav. Res. Methods, Instruments and Computer* **18** (1997) 623–632.
- [22] Heywood, C.A., Silveira, L.C. and Cowey, A. Contrast sensitivity in rats with increased or decreased numbers of retinal ganglion cells. *Exp. Brain Res.* **70** (1988) 513–526.
- [23] Innocenti, G.M., Kiper, D.C., Knyazeva, M.G. and Deonna, Th.W. On nature and limits of cortical developmental plasticity after an early lesion, in a child. *Restor. Neurol. Neurosci.* **15** (1999) 219–227.
- [24] Inoue, T., Sasaki, H., Hosokawa, M. and Fukuda, Y. Axonal regeneration of mouse retinal ganglion cells by peripheral nerve transplantation; a quantitative study. *Restor. Neurol. Neurosci.* **17** (2000) 23–29.
- [25] Kasten, E., Wüst, S., Behrens-Baumann, W. and Sabel, B.A. Computer-based training for the treatment of partial blindness. *Nature med.* **4** (1998) 1083–1087.
- [26] Kasten, E., Poggel, D., Müller-Oehring, E., Gothe, J., Schulte, T. and Sabel, B.A. (1999) Restoration of vision II: residual vision and visual field enlargements in patients with brain damage. *Restor. Neurol. Neurosci.* **15** (1999) 73–79.
- [27] Keller, J., Cerutti, D.T., Strasburger, H. and Sabel, B.A. Assessing spatial vision: automated measurements of the contrast sensitivity function in the hooded rat. *J. Neurosci Meth.* **97** (2000) 103–110.
- [28] Kerkhoff, G. Restorative and compensatory therapy approaches in cerebral blindness – a review. *Restor. Neurol. Neurosci.* **15** (1999) 255–271.
- [29] Kreutz, M.R., Bockers, T.M., Bockmann, J., Seidenbecher, C.I., Kracht, B., Vorwerk, C.K., Weise, J. and Sabel, B.A. Axonal injury alters alternative splicing of the retinal NR1 receptor: the preferential expression of the NR1b isoforms is crucial for retinal ganglion cell survival. *J. Neurosci.* **18** (1998) 8278–8291.
- [30] Lashley, K. (1939) The mechanisms of vision XVI. The function of small remnants of the visual cortex. *J. Comp. Neurol.* **70** (1939) 45–67.
- [31] Lau, K.C., So, K.-F., Cho, E.Y.P. Morphological changes of retinal ganglion cells regenerating axons along peripheral nerve grafts: a Lucifer Yellow and silver staining study. *Restor. Neurol. Neurosci.* **3** (1991) 235–246.
- [32] Linden, R., Cowey, A. and Perry, V.H. Tectal ablation at different ages in developing rat has different effects on retinal ganglion cell density but not on visual acuity. *Exp. Brain Res.* **51** (1983) 368–376.
- [33] Maxwell, W.L., Povlishock, J.T., Graham, D.L. A mechanistic analysis of nondisruptive axonal injury: a review. *J. Neurotrauma* **14** (1997) 419–440.
- [34] Maxwell, W.L., Follows, R., Ashhurst, D.E. and Berry, M. The response of the cerebral hemisphere of the rat to injury: I. the mature rat. *Phil. Trans. Soc. Lond.* **328** (1990) 479–500.
- [35] Moore, T., Rodman, H.R., Repp, A.B. and Gross, C.G. Localization of visual stimuli after striate cortex damage in monkeys: parallels with human blindsight. *Proc. Natl. Acad. Sci. USA* **92** (1995) 8215–8218.
- [36] Moore, S. and Thanos, S. Differential increases in rat retinal ganglion cell size with various methods of optic nerve lesion. *Neurosci. Lett.* **207** (1996) 117–120.
- [37] Payne, B. System-wide repercussions and adaptive plasticity: The sequelae of immature visual cortex damage. *Restor. Neurol. Neurosci.* **15** (1999) 81–106.
- [38] Povlishock, J.T., Christman, C.W. The pathobiology of traumatically induced axonal injury in animals and humans: a review of current thoughts. *J. Neurotrauma* **12** (1995) 555–564.
- [39] Quan, M.-Z., Kosaka, J., Watanabe, M., Wakabayashi, T., Fukuda, Y. Survival of axotomized retinal ganglion cells in peripheral nerve-grafted ferrets. *Invest. Ophthalmol. Vis. Sci.* **40** (1999) 2360–2366.
- [40] Rousseau, V., Engelmann, R., Sabel, B.A. Restoration of vision III: soma swelling dynamics predicts neuronal death or survival after optic nerve crush *in vivo*. *NeuroReport* **10** (1999) 3387–3391.
- [41] Sabel, B.A. Unrecognized potential of surviving neurons. Within systems plasticity, recovery of function, and the hypothesis of minimal residual structure. *Neuroscientist* **3** (1997) 366–370.
- [42] Sabel, B.A., Sautter, J., Stoehr, T. and Siliprandi, R. A behavioral model of excitotoxicity: retinal degeneration, loss of vision, and subsequent recovery after intraocular NMDA-administration in adult rats. *Exp. Brain Res.* **106** (1995) 93–105.
- [43] Sabel, B.A., Engelmann, R. and Humphrey, M.F. In vivo confocal neuroimaging (ICON) of CNS neurones. *Nature Med.* **3** (1997a) 244–247.

- [44] Sabel, B.A., Kasten, E. and Kreutz, M.R. Recovery of vision after partial visual system injury as a model of post-lesion neuroplasticity. *Adv. Neurol.* **73** (1997b) 251–276.
- [45] Sabel, B.A. Restoration of vision I: Neurobiological mechanisms of restoration and plasticity after brain damage – a review. *Restor. Neurol. Neurosci.* **15** (1999) 177–200.
- [46] Sautter, J. and Sabel, B.A. Recovery of brightness discrimination in adult rats despite progressive loss of retrogradely labelled retinal ganglion cells after controlled optic nerve crush. *Eur. J. Neurosci.* **5** (1993) 680–690.
- [47] Schmitt, U., Cross, R., Pazdernik, T.L. and Sabel, B.A. Loss and subsequent recovery of local cerebral glucose use in visual targets after controlled optic nerve crush in adult rats. *Exp. Neurol.* **139** (1996) 17–24.
- [48] Schmitt, U. and Sabel, B.A. MK-801 increases retinal ganglion cell death but reduces visual deficits after controlled optic nerve crush. *J. Neurotrauma* **13** (1996) 791–800.
- [49] Stein, D.G., Finger, S. and Hart, T. Brain damage and recovery: problems and perspectives. *Behav. Neural Biol.* **37** (1983) 185–222.
- [50] Steward, O. Assessing the functional significance of lesion-induced neuronal plasticity. *Int. Rev. Neurobiol.* **23** (1982) 197–253.
- [51] Tabata, T. and Fukuda, Y. Dendritic regrowth of retinal ganglion cells in adult rats. *NeuroReport* **3** (1992) 709–712.
- [52] Thanos, S. and Mey, J. Type-specific stabilization and target-dependent survival of regenerating ganglion cells in the retina of adult rats. *J. Neurosci.* **15** (1995) 1057–1079.
- [53] Werth, R., Moerenschlager, M. The development of visual functions in cerebrally blind children during a systematic visual field training. *Restor. Neurol. Neurosci.* **15** (1999) 229–241.
- [54] Wessinger, C.M., Fendrich, R. and Gazzaniga, M.S. Variability of residual vision in hemianopic subjects. *Restor. Neurol. Neurosci.* **15** (1999) 243–253.
- [55] Wörgötter, F., Suder, K. and Funke, K. The dynamic spatio-temporal behavior of visual responses in thalamus and cortex. *Restor. Neurol. Neurosci.* **15** (1999) 137–152.